A Model for Rate-Dependent Hysteresis in Piezoceramic Materials Operating at Low Frequencies

Ralph C. Smith,[1] Zoubeida Ounaies[2] and Robert Wieman[3]

[1,3]Center for Research in Scientific Computation, North Carolina State Univ., Raleigh, NC 27695
[2]ICASE, Mail Stop 132c, NASA Langley Research Center, Hampton, VA 23681

Abstract

This paper addresses the modeling of certain rate-dependent mechanisms which contribute to hysteresis inherent to piezoelectric materials operating at low frequencies. While quasistatic models are suitable for initial material characterization in some applications, the reduction in coercive field and polarization values which occur as frequencies increase must be accommodated to attain the full capabilities of the materials. The model employed here quantifies the hysteresis in two steps. In the first, anhysteretic polarization switching is modeled through the application of Boltzmann principles to balance the electrostatic and thermal energy. Hysteresis is then incorporated through the quantification of energy required to translate and bend domain walls pinned at inclusions inherent to the materials. The performance of the model is illustrated through a fit to low frequency data (0.1 Hz - 1 Hz) from a PZT5A wafer.

Keywords: Rate-dependent hysteresis model, piezoceramic materials

1. Introduction

The majority of currently employed models for hysteresis in ferroelectric materials are based on the assumption of static or quasistatic operating conditions. However, it has long been recognized that the polarization which is generated at a given field strength is dependent upon the rate at which the field is cycled. Hence while quasistatic models may be suitable for initial material characterization in certain applications, the incorporation of rate-dependence in the models is necessary to quantify the material behavior through its full operational range. In this paper we characterize the low frequency rate-dependent hysteresis in piezoceramic materials through a model comprised of two components: (i) A frequency-dependent anhysteretic model developed from Boltzmann principles, and (ii) Algebraic and ODE relations which quantify reversible and irreversible polarization changes due to the bending and translation of domain walls.

The dependence of the polarization, in barium titanate, on the rate at which the field is cycled was discussed in detail by Landauer et al. [11] with significant reference to observations made by Merz [12]. These references illustrate that the coercive field at which the polarization switches direction is dependent upon the time allowed for switching. As illustrated in Figure 2 of [11], the rate at which the field cycles also significantly affects the shape of the polarization curve, with the maximum polarization attained at a fixed field strength decreasing with increasing frequency.

To illustrate these phenomena in the context of piezoceramic materials, data collected from a PZT5A wafer for input fields ranging from 0.1 Hz to 1 Hz is plotted in Figure 1. A comparison between the 0.1 Hz quasistatic data and the 1 Hz data illustrates a decrease in both the coercive field and the polarization as the frequency increases. This indicates the necessity of considering the effects of rate-dependence, even at very low frequencies.

Numerous modeling strategies have been employed to quantify hysteresis in piezoelectric and ferroelectric materials. These include microscopic theories applied at the lattice or grain level [13], macroscopic theories based on

[1]Email: rsmith@eos.ncsu.edu; Telephone: 919-515-7552
[2]Email: z.ounaies@larc.nasa.gov; Telephone: 757-864-9582
[3]Email: rewieman@eos.ncsu.edu; Telephone: 919-515-2039

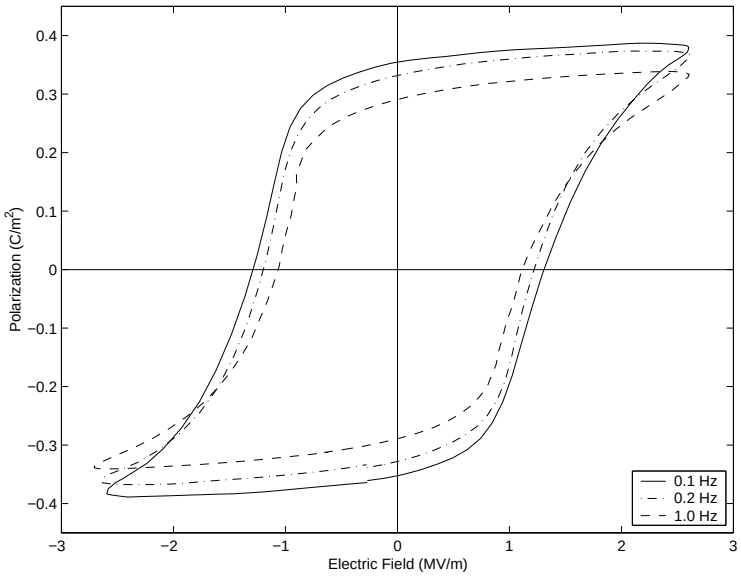

Figure 1. Rate-dependent hysteresis measured in a PZT5A wafer for input fields cycled from 0.1 Hz to 1.0 Hz.

empirical observations [4, 6, 7, 8, 9], and semi-macroscopic models which combine energy relations with macroscopic averages to quantify the bulk behavior of the material [3, 10, 15, 16, 17]. While some of these models incorporate frequency-dependence (e.g., [13, 17]), the majority of current analysis is directed toward static or quasistatic hysteresis phenomena. Moreover, a basic tenet underlying the construction of Preisach models is the assumption that the hysteresis behavior is rate independent [2]. Hence this approach will not accommodate variable frequencies of the type illustrated in Figure 1 using a single parameter set.

The model developed here is based on the approach employed in [14, 15, 16] for quasistatic regimes. The anhysteretic polarization is modeled first through the balance of electrostatic and thermal energies using Boltzmann principles. In the original formulation of the model, the anhysteretic polarization was formulated under equilibrium conditions between the field and polarization. Hysteresis was then incorporated by quantifying the irreversible and reversible changes in polarization due to domain wall movement. The modification of the model considered here is based on probabilistic arguments which ascertain the rate-dependence of the anhysteretic polarization. The resulting model yields the decrease in polarization observed in piezoceramic materials as the drive frequency increases. Hence it quantifies the effects observed in Figure 1. Finally, this model reduces to the quasistatic models in [14, 15, 16] when frequencies are limited to zero.

The quasistatic model from [14, 15, 16] is summarized in Section 2 to illustrate the methodology and to indicate necessary modifications. The rate-dependent model is then developed in Section 3 and the performance of the model is illustrated in Section 4 through a comparison of the model prediction with the experimental data plotted in Figure 1.

2. Quasistatic Model

To illustrate the modeling approach and indicate components which must be modified, we summarize the model developed in [14, 15, 16] for hysteresis in quasistatic regimes. As indicated earlier, the model is comprised of two components. The first models the anhysteretic polarization which is due to polar switching in addition to domain rotation at high field levels. Under certain conditions, the anhysteretic polarization is multivalued and hence incorporates a form of hysteresis. The transition between remanence and the coercive point is typically steeper than that observed in most ferroelectric materials, however, due to their polycrystalline nature and the inhibition of domain wall movement due to inclusions inherent to the materials. The latter effects are quantified through the consideration of energy required to bend and translate domain walls pinned at inclusions in the material. The combined model characterizes the nonlinear and hysteretic relation between the input field E and the polarization P generated in the material.

The anhysteretic polarization for both quasistatic and dynamic regimes is modeled through the balance of the electrostatic and thermal energy using Boltzmann principles. For a dipole $\mathbf{p}$ in an electric field $\mathbf{E}$, the potential energy is

$$\mathcal{E} = -\mathbf{p} \cdot \mathbf{E} = -pE\cos(\theta) \tag{1}$$

where $p = |\mathbf{p}|$ and $E = |\mathbf{E}|$. The thermal energy at temperature T is given by $\mathcal{E}_T = k_B T$ where k_B denotes Boltzmann's constant. The probability that a dipole occupies the energy state $\mathcal{E}$ is then specified through Boltzmann statistics as

$$\mu(\mathcal{E}) = Ce^{-\mathcal{E}/k_B T} \tag{2}$$

where the parameter C is chosen to ensure that integration over all possible dipole configurations yields the total number N of moments per unit volume. The assumptions specifying possible moment orientations determines the form of the anhysteretic model.

The simplest model results from the assumption that dipoles can be oriented only in the direction of the electric field or opposite to it. If we let N_+ and N_- respectively denote the number of dipoles oriented with and opposing the field, then the application of (2) yields

$$N_+ = Ce^{pE/k_B T} \quad , \quad N_- = Ce^{-pE/k_B T}. \tag{3}$$

Since $N = N_+ + N_-$, it then follows that

$$N = 2C\cosh\left(\frac{pE}{k_B T}\right). \tag{4}$$

The polarization for this configuration is given by

$$P = pN_+ - pN_- = 2pC\sinh\left(\frac{pE}{k_B T}\right)$$

which yields the Ising spin relation

$$P = pN\tanh\left(\frac{pE}{k_B T}\right) \tag{5}$$

relating E and P.

As detailed in [15], the anhysteretic polarization saturates to the value P_s for increasing field inputs. Furthermore the relation (5) ignores the interaction with neighboring domains as well as electromechanical inputs due to applied stresses. The inclusion of these mechanisms yields the anhysteretic relation

$$P_{an} = P_s\tanh\left(\frac{E_e}{a}\right) \tag{6}$$

where

$$E_e = E + \alpha P + P_\sigma \tag{7}$$

denotes the effective field acting on the domain. The parameter α quantifies the degree of interdomain coupling while P_σ incorporates field contributions from an applied stress σ. The parameter a quantifies a form of temperature-dependence due to the thermal energy [15]. For material characterization, the parameters P_s, α and a are estimated either from asymptotic relations or a least squares fit to data [16].

A second anhysteretic model is obtained under the assumption that the dipoles can orient uniformly in all directions. Integration and scaling for this case yields the Langevin model

$$P_{an} = P_s\left[\coth\left(\frac{E_e}{a}\right) - \left(\frac{a}{E_e}\right)\right]. \tag{8}$$

As illustrated in [15], the Langevin model saturates less quickly than the Ising spin model since dipoles have more freedom concerning the directions in which they can orient. Both models have been employed to characterize the anhysteretic behavior of ferroelectric and piezoceramic materials.

The second component of the hysteresis model incorporates the energy required to translate and bend domain walls pinned at inclusions inherent to the material. As detailed in [15], this respectively yields an irreversible

component P_{irr} and reversible component P_{rev} to the polarization. The quantification of energy required to break pinning sites yields the differential equation

$$\frac{dP_{irr}}{dE} = \widetilde{\delta}\frac{P_{an} - P_{irr}}{k\delta - \alpha\,(P_{an} - P_{irr})} \tag{9}$$

specifying the irreversible polarization. The parameter $\delta = \text{sign}(dE)$ ensures that the energy required to break pinning sites always opposes changes in polarization. The physical observation that polarization changes after a reversal in field direction are reversible motivates the incorporation of the parameter

$$\widetilde{\delta} = \begin{cases} 1\ , & \{dE < 0 \text{ and } P > P_{an}\} \text{ or } \{dE < 0 \text{ and } P > P_{an}\} \\ 0\ , & \text{otherwise} \end{cases} .$$

Finally, the parameter k, which quantifies the average energy required to reorient domains, is demonstrated in [16] to be asymptotically approximated by the coercive field E_c in soft materials.

The second component of the polarization is the reversible polarization which models the effects of domain wall bending. To first approximation, this is modeled by the relation

$$P_{rev} = c(P_{an} - P_{irr}) \tag{10}$$

where c is a parameter which must be estimated for the specific application.

The total polarization is then given by

$$P = P_{rev} + P_{irr}\ . \tag{11}$$

To implement the model, the effective field for a given field and irreversible polarization level is computed using (7). This effective field value is then employed in either (6) or (8) to compute the corresponding anhysteretic polarization. The subsequent irreversible polarization is determined by numerically integrating (9) and the total polarization is specified by (11).

3. Time-Dependent Model

The model summarized in Section 2 is derived under the assumption of equilibrium conditions when employing the electrostatic potential energy relation (1) to derive the model for the anhysteretic polarization along with the energy required to reorient dipoles and hence break pinning sites. This assumption is valid under static or quasistatic operating conditions but omits rate-dependent mechanisms which are significant even at low frequencies. In this section, we derive a model for the anhysteretic polarization which incorporates this rate-dependence and reduces to the Ising spin model as the frequency is limited to zero. This quantifies a significant component of the rate-dependent behavior observed in Figure 1.

3.1. Anhysteretic Polarization

To derive the anhysteretic model, we consider the material to be comprised of a lattice of cells with each cell having a dipole moment that is aligned either in the direction of the field or opposite to it. This is the same assumption made when deriving the Ising spin model in Section 2 and is analogous to the regimes considered in [1, pages 69-71], [5, pages 104-106] and [19, pages 370-373]. The number of cells aligned in the direction of the applied field at time t is denoted by $N_1(t)$ and $N_2(t)$ denotes the number of cells whose dipole moment is oriented in the opposite direction.

The potential energy associated with the two equilibria is depicted in Figure 2. In the absence of an applied field, any interchange of dipole orientations is due to thermal fluctuations, whereas dipoles have a higher probability of overcoming the energy barrier and the number $N_1(t)$ increases in the presence of an applied field E. To quantify this increase, we let w_{21} denote the probability that one cell, considered for one second, switches orientation into the field direction and let w_{12} denote the probability that a dipole switches in the opposite direction due to thermal excitation. The change in the number of cells having a specific orientation is then determined by the equations

$$\frac{dN_1}{dt} = -w_{12}N_1 + w_{21}N_2$$

$$\frac{dN_2}{dt} = w_{12}N_1 - w_{21}N_2\,.$$

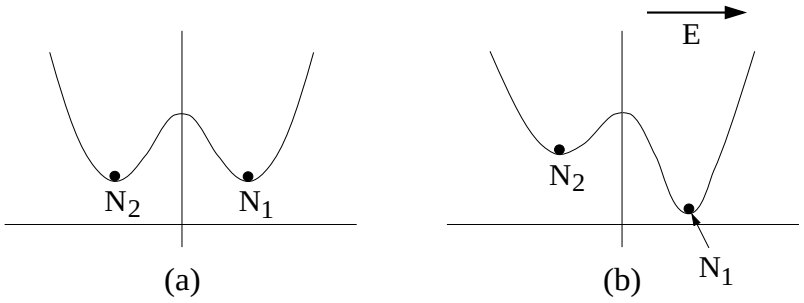

Figure 2. The double potential well associated with the two equilibria; (a) No applied field, (b) An applied field E.

At equilibrium, the conditions $\frac{dN_1}{dt} = \frac{dN_2}{dt} = 0$ yield the requirement

$$\frac{w_{12}}{w_{21}} = \frac{N_2}{N_1}. \tag{12}$$

In this case, the Boltzmann relation (2) holds and

$$\begin{aligned} N_1 &= Ce^{pE/k_BT} \\ N_2 &= Ce^{-pE/k_BT} \end{aligned} \tag{13}$$

where, from (4), the parameter C is specified by $C(E,T) = \frac{N}{2\cosh(pE/k_BT)}$. A comparison of (13) with (3) illustrates that the Ising spin distribution results when the time-dependent system considered here is allowed to reach equilibrium. Given the form of N_1 and N_2, the probabilities can be expressed as

$$w_{12} = \frac{1}{2\tau}e^{-pE/k_BT}$$

$$w_{21} = \frac{1}{2\tau}e^{pE/k_BT}$$

where $\tau(E,T)$ is an arbitrary function of E and T. To determine the form of $\tau(E,T)$, we note that when the system is not in equilibrium, and hence $\frac{dN_1}{dt} \neq 0$, the probability that a cell switches orientation is nonzero. Hence

$$w_{12} + w_{21} = \frac{1}{\tau_1}$$

which yields the condition

$$\tau(E,T) = \tau_1(E,T)\ \cosh\left(\frac{pE}{k_BT}\right). \tag{14}$$

The parameter τ_1 is, in general, also a function of E and T. For the model comparison to PZT5A data presented in Section 4, we consider isothermal conditions and assume sufficiently small field dependence to justify considering τ_1 as constant. In general applications, however, the determination of mechanisms for determining the field and temperature dependence in τ_1 may improve the accuracy of the model.

We now consider the solution of the resulting system

$$\begin{aligned} \frac{dN_1}{dt} &= -\frac{1}{2\tau}e^{-pE/k_BT}N_1 + \frac{1}{2\tau}e^{pE/k_BT}N_2 \\ \frac{dN_2}{dt} &= \frac{1}{2\tau}e^{-pE/k_BT}N_1 - \frac{1}{2\tau}e^{pE/k_BT}N_2 \end{aligned} \tag{15}$$

under two sets of assumptions regarding the input field E. For a general E, the solution of (15) is

$$N_1(t) = k_1 + k_2e^{-(t/\tau)\cosh(pE/k_BT)}$$

$$N_2(t) = k_1e^{-2pE/k_BT} - k_2e^{-(t/\tau)\cosh(pE/k_BT)}.$$

To determine the integration constants k_1 and k_2, we consider the limiting behavior as $t \to 0$ and $t \to \infty$. As $t \to \infty$, the distribution of dipoles limits to the equilibrium case (13) modeled by the Ising spin relation. This yields

$$k_1 = Ce^{pE/k_BT} .$$

The enforcement of equal initial dipole distributions, $N_1(0) = N_2(0)$, requires that

$$k_2 = C \sinh\left(\frac{pE}{k_BT}\right) .$$

The final distribution of dipoles at a given field level is then

$$\begin{aligned} N_1(t) &= Ce^{pE/k_BT} + C \sinh\left(\frac{pE}{k_BT}\right) e^{-t/\tau_1} \\ N_2(t) &= Ce^{-pE/k_BT} - C \sinh\left(\frac{pE}{k_BT}\right) e^{-t/\tau_1} \end{aligned} \tag{16}$$

where (14) was used to eliminate $\tau(E,T)$.

The polarization generated by this dipole configuration is specified through the relation

$$\begin{aligned} P(t) &= pN_1(t) - pN_2(t) \\ &= 2pC \sinh\left(\frac{pE}{k_BT}\right)\left[1 - e^{-t/\tau_1}\right] \\ &= pN \tanh\left(\frac{pE}{k_BT}\right)\left[1 - e^{-t/\tau_1}\right] . \end{aligned} \tag{17}$$

For the effective field $E_e = E + \alpha P + P_\sigma$ introduced in (7), this yields the rate-dependent anhysteretic polarization model

$$P_{an}(t) = P_s \tanh\left(\frac{E_e}{a}\right)\left[1 - e^{-t/\tau_1}\right] . \tag{18}$$

A comparison of (18) with the Ising spin model (6) indicates that the latter is obtained as $t \to \infty$.

We consider now the response of the anhysteretic polarization to a periodic input field

$$E(t) = E_0 e^{i\omega t} . \tag{19}$$

To accommodate the periodicity, we consider solutions of the form

$$\begin{aligned} N_1(t) &= N_0 + \nu_0 e^{i\omega t} \\ N_2(t) &= N_0 - \nu_0 e^{i\omega t} . \end{aligned}$$

The substitution of these expressions into (15) and consolidation of terms yields

$$\nu_0 = \frac{N_0}{1 + i\omega\tau_1} \tanh\left(\frac{pE(t)}{k_BT}\right) e^{-i\omega t}$$

where $E(t)$ is of the form assumed in (19). The resulting polarization is then

$$\begin{aligned} P(t) &= pN_1(t) - pN_2(t) \\ &= \frac{pN}{1 + i\omega\tau_1} \tanh\left(\frac{pE(t)}{k_BT}\right) . \end{aligned}$$

The isolation of the real component of the polarization, enforcement of saturation criteria, and the incorporation of the effective field E_e then yields the frequency-dependent anhysteretic relation

$$P_{an}(t) = \frac{P_s}{1 + \omega\tau_1} \tanh\left(\frac{E_e}{a}\right) . \tag{20}$$

We first note that as $\omega \to 0$, this expression reduces to the Ising spin model (6). In this formulation, it can also be observed that the parameter τ_1 acts as a relaxation time. While τ_1 is considered constant for the example in Section 4, it is in general a function of both E and T. Finally, we note that for increasing frequencies, the expression incorporates the decrease in polarization observed in the data plotted in Figure 1.

3.2. Hysteresis Model

The expression (20) provides a frequency-dependent model for the anhysteretic polarization. This relation is combined with the expression (9) for the irreversible polarization P_{irr} and (10) for the reversible polarization P_{rev} to obtain a frequency-dependent model for the total polarization. We note that the construction of the model in this manner neglects the quantification of rate-dependence in the energy required to bend domain walls or break pinning sites, thus rendering the model accurate only at low frequencies. The incorporation of these latter effects is under investigation and will be reported in a future work. An example illustrating the performance of the model at low frequencies (0.1 Hz and 1.0 Hz) is provided in the next section.

4. Model Validation

The model developed in Section 3 quantifies both the hysteresis inherent to the E-P relation and the decrease in polarization which occurs when the frequency of the input field is increased from quasistatic to low frequency regimes. To illustrate its capabilities, we consider the characterization of polarization generated in a PZT5A wafer in response to a 2.5 MV/m input field at frequencies ranging from 0.1 Hz to 1.0 Hz. A constant temperature was maintained to ensure isothermal conditions.

The parameters $a = 1.8 \times 10^6$ C/m, $\alpha = 3.6 \times 10^6$ Vm/C, $k = 1.65 \times 10^6$ C/m^2, $c = 0.1$, $P_s = 0.52$ C/m^2 and $\tau_1 = 0.16$ were obtained through a least squares fit to the data collected at 0.1 Hz. Once obtained, these parameters were held fixed and variations in operating regimes were incorporated through the magnitude E_0 and frequency ω of the input field.

The model predictions at 0.1 Hz and 1.0 Hz are compared with the experimental data in Figure 3. It is observed that the model very accurately quantifies the data at 0.1 Hz which is the regime in which the parameters were estimated. The model also accurately predicts the decrease in polarization at 1 Hz, but does not yet incorporate the decrease in the coercive field which occurs as frequency increases. The incorporation of rate-dependence in the energy required to bend and translate domain walls is under current investigation.

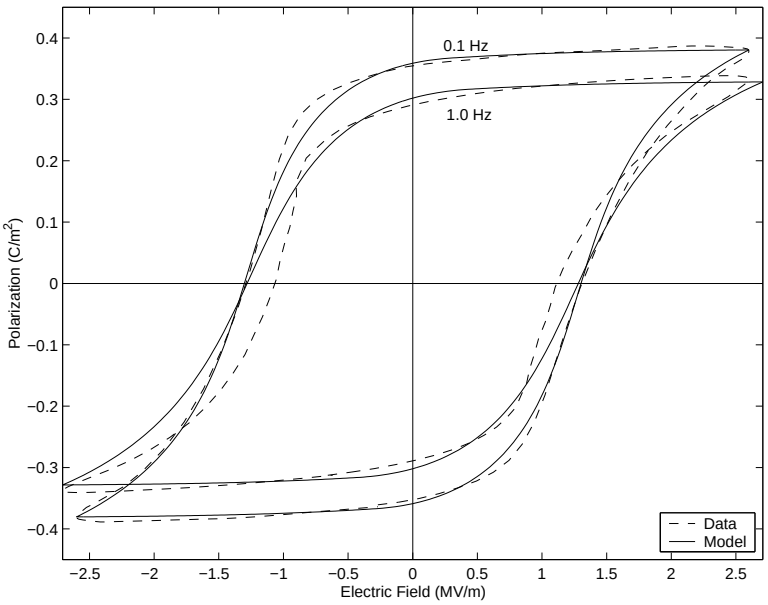

Figure 3. Model fit to 0.1 Hz and 1.0 Hz PZT5A data with the parameters $a = 1.8 \times 10^6$ C/m, $\alpha = 3.6 \times 10^6$ Vm/C, $k = 1.65 \times 10^6$ C/m^2, $c = 0.1$, $P_s = 0.52$ C/m^2 and $\tau_1 = 0.16$

5. Concluding Remarks

This paper addresses the quantification of certain rate-dependent mechanisms inherent to the hysteretic relation between the field applied to a piezoceramic material and the resulting polarization. The analysis presented here focuses primarily on the reduction in polarization which occurs as frequencies increase from quasistatic levels to low frequency regimes. This is modeled by determining the probability that dipoles achieve the energy required to overcome energy barriers and switch orientation when an external field is applied. The resulting model, which quantifies the anhysteretic polarization exhibited by the material, reduces to the Ising spin model when the driving frequency is reduced to quasistatic levels. This anhysteretic relation is then combined with expressions quantifying domain wall losses to provide a model which characterizes the hysteresis exhibited by the material.

In its current formulation, the model is restricted to low frequency regimes since it does not yet incorporate rate-dependent mechanisms for quantifying the energy required to reorient dipoles when translating domain walls. The extension of the model to include these mechanisms is necessary in order to increase the applicable frequency range of the model and is under current investigation.

Acknowledgements

The research of R.C.S. was supported in part by the Air Force Office of Scientific Research under the grant AFOSR-F49620-98-1-0180.

References

[1] J.C. Anderson, *Dielectrics*, Reinhold Publishing Corporation, New York, 1964.

[2] M. Brokate and J. Sprekels, *Hysteresis and Phase Transitions*, Springer, New York, 1996.

[3] W. Chen and C.S. Lynch, "A model for simulating polarization switching and AF-F phase changes in ferroelectric ceramics," *Journal of Intelligent Material Systems and Structures*, 9, pp. 427-431, 1998.

[4] P.J. Chen and S.T. Montgomery, "A macroscopic theory for the existence of the hysteresis and butterfly loops in ferroelectricity," *Ferroelectrics*, 23, pp. 199-208, 1980.

[5] P. Debye, *Polar Molecules*, The Chemical Catalogue Company, New York, 1929.

[6] W.S. Galinaitis and R.C. Rogers, "Compensation for hysteresis using bivariate Preisach Models," SPIE Smart Structures and Materials, 1997, Mathematics and Control in Smart Structures, San Diego, CA, 1997.

[7] W.S. Galinaitis and R.C. Rogers, "Control of a hysteretic actuator using inverse hysteresis compensation," SPIE Smart Structures and Materials, 1998, Mathematics and Control in Smart Structures, San Diego, CA, 1998.

[8] P. Ge and M. Jouaneh, "Modeling hysteresis in piezoceramic actuators," *Precision Engineering*, 17, pp. 211-221, 1995.

[9] P. Ge and M. Jouaneh, "Tracking control of a piezoceramic actuator," *IEEE Transactions on Control Systems Technology*, 4(3), pp. 209-216, 1996.

[10] L. Huang and H.F. Tiersten, "An analytic description of slow hysteresis in polarized ferroelectric ceramic actuators," *Journal of Intelligent Material Systems and Structures*, 9, pp. 417-426, 1998.

[11] R. Landauer, D.R. Young and M.E. Drougard, "Polarization reversal in the barium titanate hysteresis loop," *Journal of Applied Physics*, 27(7), pp. 752-758, 1956.

[12] W.J. Merz, "Domain formation and domain wall motions in ferroelectric $BaTiO_3$ single crystals," *Physical Review*, 95(3), pp. 690-698, 1954.

[13] M. Omura, H. Adachi and Y. Ishibashi, "Simulations of ferroelectric characteristics using a one-dimensional lattice model," *Japanese Journal of Applied Physics*, 30(9B), pp. 2384-2387, 1991.

[14] R.C. Smith and C.L. Hom, "A domain wall model for ferroelectric hysteresis," SPIE Conference on Mathematics and Control in Smart Structures, SPIE Volume 3667, Newport Beach, CA, March 1-4, pp. 150-161, 1999.

[15] R.C. Smith and C.L. Hom, "A domain wall theory for ferroelectric hysteresis," CRSC Technical Report CRSC-TR99-1; *Journal of Intelligent Material Systems and Structures*, to appear.

[16] R.C. Smith and Z. Ounaies, "A domain wall model for hysteresis in piezoelectric materials," CRSC Technical Report CRSC-TR99-33; *Journal of Intelligent Material Systems and Structures*, submitted.

[17] I.K. Yoo and S.B. Desu, "Modeling of hysteresis in ferroelectric thin films," *Philosophical Magazine B*, 69(3), pp. 461-469, 1994.

[18] X.D. Zhang and C.A. Rogers, "A macroscopic phenomenological formulation for coupled electromechanical effects in piezoelectricity," *Journal of Intelligent Material Systems and Structures*, 4, pp. 307-316, 1993.

[19] I.S. Zheludev, *Physics of Crystalline Dielectrics. Volume 2: Electrical Properties*, Translated by A. Tybulewicz, Plenum Press, New York, 1971.